Manganese triggers phosphorylation-mediated endocytosis of the Arabidopsis metal transporter NRAMP1

Loren Castaings, Carine Alcon, Thibault Kosuth, David Correia, Catherine Curie

DR CATHERINE CURIE (Orcid ID : 0000-0002-8884-1175)

Article type : Original Article

Manganese triggers phosphorylation-mediated endocytosis of the Arabidopsis metal transporter NRAMP1

Loren Castaings[a], Carine Alcon, Thibault Kosuth, David Correia, & Catherine Curie[a]

BPMP, Univ Montpellier, CNRS, INRAE, Institut Agro, Montpellier, France.

[a]Corresponding authors

Running Title Phosphorylation-mediated cycling of NRAMP1

Key words

Manganese, Transport, Endocytosis, Membrane traffic, Phosphorylation, *Arabidopsis thaliana*

Contact

catherine.curie@supagro.fr

loren.castaings@supagro.fr

Abstract

The NATURAL RESISTANCE ASSOCIATED MACROPHAGE PROTEIN 1 (NRAMP1) transporter guarantees survival of the plant to Mn deficiency by mediating Mn entry into root cells. Unlike other high-affinity metal transporters, NRAMP1 is only slightly regulated at the transcriptional level. We show here that adequate Mn content in tissues is safeguarded through a tight control of the amount of NRAMP1 present at the surface of root cells. Depending on Mn availability, an NRAMP1-GFP fusion protein cycles dynamically between the plasma membrane (PM) and endosomal compartments. This involves a clathrin-mediated endocytosis pathway since disrupting the latter in auxilin-overexpressor lines prevents NRAMP1 internalization. Mutation of the phosphorylated serine residues 20, 22 and 24 in the cytosol-exposed N-terminus of NRAMP1 alters its membrane distribution. Indeed, a phosphodead mutation stabilizes NRAMP1 at the PM regardless of the Mn regime and dramatically reduces plant tolerance to Mn toxicity. Conversely a phosphomimetic mutant is constitutively internalized into endosomes. Together these data establish that phosphorylation of NRAMP1 is the trigger for its Mn-induced endocytosis and represents the main level of regulation of this transporter. Furthermore, the extent of Mn toxicity observed when interrupting NRAMP1 membrane cycling undermines the dogma in which Mn is only marginally toxic to plants.

Introduction

Manganese (Mn) is required in minute amounts for plant growth. Yet Mn availability in soils can be insufficient in conditions of high pH or particular microbial activity that favor chemical oxidation of Mn^{2+} into Mn oxides, which are not usable by the plant. Root responses such as exudation of protons and organic acids, which lower soil pH, also strongly influence the geochemistry of Mn (Geszvain *et al.*, 2012; Sparrow and Uren, 2014). In plants, Mn is a cofactor of many cellular proteins among which two are of considerable importance: the oxygen evolving complex of photosystem II, that catalyzes the water splitting reaction during photosynthesis, and the mitochondrial superoxide dismutase, which converts toxic superoxide ions into less toxic hydrogen peroxide and dioxygen. Therefore, Mn deficiency disorders decrease photosynthesis efficiency and predispose plants to pathogens' attack by affecting the antioxidant defenses, eventually leading to yield loss. Visual Mn deficiency symptoms are mild chlorosis and, under drastic starvation, necrosis on leaves (Marschner, 2012). On the other hand, Mn excess, occurring mainly in acid soils, is toxic to plants. Excessive amount of Mn disrupts physiological functions, triggering reactive oxygen species production and impairing photosynthesis activity. Mn excess also provokes secondary deficiencies of other nutrients such as calcium (Ca), magnesium (Mg), iron (Fe) or zinc (Zn) due to an inhibition of their uptake at the plasma membrane or a competition at the cellular level (de Varennes *et al.*, 2001; Horst, 1988). Mn toxicity symptoms include chlorosis of the young leaves, necrotic spots on mature leaves and crinkled leaves, ultimately reducing plant growth (for review, see (Li *et al.*, 2019). Preventing Mn overload and controlling Mn uptake is therefore crucial for plant health.

In substrates with low Mn availability, Mn usually enters the plant via transporters of the Natural Resistance Associated Macrophage Protein (NRAMP) family. Arabidopsis NRAMP1 and rice NRAMP5 are located at the surface of root cells where they mediate Mn uptake with an affinity for Mn in the submicromolar range (Cailliatte *et al*., 2010; Ishimaru *et al.*, 2012; Sasaki *et al.*, 2012). Many metal transporters have a broad substrate specificity. The plasma-membrane IRT1 transporter facilitates ferrous iron (Fe^{2+}) acquisition but can also transport other metals including Mn (Eide *et al.*, 1996; Ishimaru *et al.*, 2006; Vert *et al.*, 2002). Simultaneous inactivation of NRAMP1 and IRT1 in Arabidopsis provoked a dramatic loss of plant Mn content in Mn replete conditions, indicating overlapping activity of the two transporters in conditions of medium affinity range (Castaings *et al.*, 2016). In barley, in which Mn deficiency is a serious disorder (Pedas *et al.*,

2005; Schmidt *et al.*, 2016), both NRAMP and IRT1 homologs contribute to plant Mn acquisition and strikingly show a strict specificity for Mn, contrary to the majority of their homologs in other species. Knocking down HvNRAMP5 or HvIRT1 in barley altered Mn uptake and/or root-to-shoot translocation but did not disturb Fe or Zn homeostasis (Long *et al.*, 2018; Wu *et al.*, 2016). HvIRT1, but not HvNRAMP5, is upregulated by Mn deficiency at the transcriptional level (Long *et al.*, 2018). So if the dominant Mn transporter in Arabidopsis is NRAMP1 under Mn deficiency, it appears to be both HvNRAMP5 and HvIRT1 in barley.

NRAMP transporters are remarkably conserved across kingdoms, with members described from bacteria to animals. All of them have the ability to transport Fe and Mn but have a marked physiological preference for one or the other metal depending on the organism. The vast majority of the NRAMPs are regulated by their substrate, however the mode of regulation, when known, is extremely diverse. *MntH*, encoding the bacterial NRAMP homolog, is transcriptionally repressed by the Mn^{2+}-dependent repressor MntR ((Lieser *et al.*, 2003); for a review see (Papp-Wallace and Maguire, 2006)). In mammals, NRAMP2/DMT1/DCT1/SLC11A2 mediates dietary uptake of Fe at the duodenum brush border and in peripheral tissues. It is controlled by the body Fe status at the transcriptional, post-transcriptional and post-translational levels (Yanatori and Kishi, 2019). In yeast, one of the three NRAMP homologs, Smf1p, encodes a plasma membrane high-affinity Mn transporter, which is primarily regulated by ubiquitination-triggered endocytosis (Eguez *et al.*, 2004). This mechanism, including the family of E3 ubiquitin ligase and adaptors involved (Liu and Culotta, 1999; Stimpson *et al.*, 2006), has been conserved in mammals and regulates the endocytic degradation of DMT1 (Foot *et al.*, 2008).

To meet the plant demand, genes encoding high affinity transporters of nutrients are often regulated by their substrate at the transcriptional level, being generally actively transcribed in response to nutrient limitation. More recently, additional levels of control have been described to maintain nutrient homeostasis. These include mRNA stability as well as protein membrane localization and polarity. For instance, transcripts of the boron (B) transporter gene *NIP5;1* contain an upstream open reading frame, which mediates mRNA degradation under high B conditions (Tanako *et al.*, 2016). In addition, there is a growing number of studies indicating that plant transporters are actively removed from the cell surface and sorted to the vacuole for degradation, often through ubiquitin-mediated endocytosis. This was reported, among others, for

the B transporter AtBOR1, the Fe transporter IRT1 or the phosphate transporter PHT1;1 (Kasai *et al.*, 2011; Barberon *et al.*, 2011; Shin *et al.*, 2013; Lin *et al.*, 2013).

In this work, we have dissected the regulation of Arabidopsis NRAMP1. Previously, we reported that Mn deficiency induces *NRAMP1* gene expression at the transcriptional level, albeit to a moderate extent (Cailliatte *et al.*, 2010; Castaings *et al.*, 2016). We have now uncovered that the NRAMP1 protein dramatically responds to Mn availability by cycling dynamically between the plasma membrane and internal vesicular compartments. NRAMP1 removal from the cell surface requires a step of phosphorylation involving N-terminal serine residues prior to clathrin-dependent endocytosis. Disturbing this process provokes Mn toxicity, confirming that this post-translational regulation of NRAMP1 acts as a safeguard against excess Mn entry in the root.

Results

Manganese availability does not impact NRAMP1-GFP protein steady state level

Given that changes in Mn availability have little impact on NRAMP1 transcript level (Cailliatte *et al.*, 2010; Castaings *et al.*, 2016), we investigated whether NRAMP1 was regulated at the post-transcriptional level. To assess protein accumulation independently of the Mn-dependent transcriptional regulation of NRAMP1, we used a transgenic line expressing the NRAMP1-GFP translational fusion under the control of the constitutive CaMV 35S promoter in the *nramp1-1* mutant background (*nramp1-1* 35S:NRAMP1-GFP, called the NRAMP1-GFP line throughout the paper). This construct successfully rescues hypersensitivity of *nramp1-1* to Mn deficiency, indicating that the NRAMP1-GFP fusion protein is functional (Cailliatte *et al.*, 2010). We evaluated the influence of Mn nutrition on NRAMP1-GFP accumulation by immunoblot analysis with anti-GFP antibodies. Plants were grown for 7 days under Mn deficiency to optimize NRAMP1 production. Plants were then either exposed to a toxic concentration of 2 mM Mn or kept under Mn deficiency for a length of time varying from 3 h, 6 h and 24 h in the presence of cycloheximide to follow the fate of pre-existing NRAMP1-GFP. The steady state level of NRAMP1-GFP protein was essentially unaffected over the 24 h treatment (Figure S1). We concluded that the accumulation of NRAMP1-GFP protein in our line is not regulated by Mn availability.

Mn availability impacts NRAMP1-GFP membrane localization

NRAMP1 was shown in a previous study to have a dual localization at the plasma membrane (PM) and in endosomal vesicles from both the trans-Golgi / early endosomes network (TGN/EE) and the late endosome/ multivesicular bodies (LE/MVB) (Agorio et al., 2017). As expected, when NRAMP1-GFP plants were grown in Mn-replete conditions, the GFP fluorescence was distributed between PM and intracellular vesicles (Figure 1a, d). When plants were grown in the absence of Mn however, intracellular signal entirely disappeared while fluorescence at the PM increased (Figure 1b, e, g), indicating that Mn deficiency triggers redistribution of NRAMP1-GFP to the PM. On the contrary, treating Mn-starved plants with an excess amount of Mn for 1h dramatically increased the proportion of NRAMP1-GFP protein inside the cell to the detriment of its presence at the PM (Figure 1c, f). To address the specificity of the NRAMP1 dynamic response to Mn, we submitted a line expressing the auxin carrier PIN2-GFP to a similar Mn stress. In contrast to NRAMP1-GFP that is internalized upon Mn excess, PIN2-GFP stayed at the cell surface irrespective of the Mn treatment (Figure S2). We therefore concluded that an excess of Mn does not affect the localization of PM proteins in general but specifically triggers NRAMP1 internalization. To determine the nature of NRAMP1-GFP-containing vesicles upon Mn resupply, we carried out colocalization experiments by crossing the NRAMP1-GFP line with Arabidopsis lines expressing the endosomal markers mCherry-VTI12 and mCherry-ARA7, which typically label TGN/EE and MVB compartments respectively. In response to Mn excess, NRAMP1-GFP showed a high degree of colocalization with mCherry-VTI12 and a rather moderate one with mCherry-ARA7 (Figure S3). Since besides its main localization in PVC, ARA7 is also localized in TGN (Ito et al., 2016){Ito, 2016 #1778}, our observations suggest that once NRAMP1 is internalized from the PM, it is sorted out mostly to the TGN/EE endosomal compartment. We concluded from these experiments that the dynamic cycling of NRAMP1 between PM and endomembrane compartments responds to the amount of Mn available to the plant.

Interfering with clathrin-mediated endocytosis prevents NRAMP1 internalization

The internal localization of NRAMP1-GFP observed upon Mn resupply could be caused either by an inhibition of protein secretion to the PM, or by a higher rate of internalization of the protein from the PM through rapid endocytosis. Clathrin-mediated endocytosis (CME) is not only the predominant endocytic mechanism in plants, but it was also recently reported to modulate the amount of several transporters at the PM. We therefore tested the possibility that exposure to Mn

excess triggers CME of NRAMP1-GFP by investigating the impact of interfering with CME on NRAMP1-GFP localization. The NRAMP1-GFP line was crossed with a conditional AUXILIN-LIKE 2 overexpressor line (Adamowski et al., 2018). AUXILIN acting as a clathrin uncoating factor, overexpression of AUXILIN-LIKE 2 results in inhibition of endocytosis by blocking clathrin recruitment at the PM (Adamowski et al., 2018). In non-inducing conditions, where the *AUXILIN-LIKE 2* transgene is not expressed, NRAMP1-GFP was expectedly observed for the most part in endomembrane compartments and showed almost no signal at the PM under high Mn exposure (Figure 2a-c). On the contrary, when *AUXILIN-LIKE 2* expression was induced by the oestradiol treatment, NRAMP1-GFP fluorescence was no longer visible in endosomes after 1h of Mn exposure but instead fully colocalized with the PM as shown by the overlay with the FM4-64 signal (Figure 2d-f). Thus interfering with CME stabilized NRAMP1-GFP at the PM by preventing its internalization under Mn stress. We concluded that the Mn-regulated dynamic cycling of NRAMP1 between PM and endosomes involves an endocytic event depending on clathrin.

Phosphorylation controls endocytosis of NRAMP1-GFP

Trafficking of PM proteins is known to be triggered by post-translational modification marks including phosphorylation. NRAMP1 contains 9 predicted phosphorylated residues, among which a cluster of three serines at positions 20, 22 and 24 at the N-terminal part of the protein. Two of them, serine 20 and 22 were found to be phosphorylated in Arabidopsis published proteomes (Figure S4). To investigate the role of N-terminal serines (S) in NRAMP1 cycling in response to Mn, S_{20}, S_{22} and S_{24} were simultaneously mutated either into the non-phosphorylatable alanine (A) residue ($S_{20,22,24}A$) or, to mimic phosphorylation, into the aspartic acid (D) residue ($S_{20,22,24}D$). GFP fusions of these mutated NRAMP1 proteins were stably transformed in the *nramp1-1* mutant. Membrane distribution of these NRAMP1 variants was assessed by confocal microscopy observation in the corresponding NRAMP1 $S_{20,22,24}A$-GFP and NRAMP1 $S_{20,22,24}D$-GFP transgenic lines. Experimental conditions were designed as to allow visualization of protein movement, if any, in both directions: relocation to the PM or internalization to the endosomes. To that aim, plants were grown under Mn limitation (0.2 µM), rather than in Mn-free medium as in Figure 1, so that NRAMP1-GFP distribution was shared between PM and endosomes (Figure 3a), prior to a 1h exposure to Mn excess. The wild-type control NRAMP1-GFP behaved as expected in response to Mn by shifting its localization toward the endosomes (Figure 3b). The phosphodead

mutations led to stabilization of NRAMP1-GFP at the PM regardless of the Mn concentration in the culture medium (Figure 3c, d). This indicated that one or several of these serines is/are required for endocytosis of the protein in response to Mn. Conversely, the phosphomimetic mutations resulted in constitutive intracellular targeting of NRAMP1-GFP protein in both Mn regimes (Figure 3e, f). None of these two mutations impaired the capacity of NRAMP1-GFP to rescue *nramp1-1* hypersensitivity to Mn deficiency (Figure 4, compare panels d and e with panel b). Therefore, the serines 20, 22 and 24 are dispensable for NRAMP1 transport activity but they control the protein subcellular dynamics. Furthermore, although the phospho-mimetic isoform was no longer detected at the PM, its ability to rescue *nramp1-1* hypersensitivity to Mn deficiency indicated that its secretion to the PM remained unaffected. Rather, mimicking phosphorylation appeared to accelerate the rate of protein internalization. Based on colocalization with endomembrane markers, NRAMP1 $S_{20,\ 22,\ 24}$D-GFP protein was observed in the same cell compartments as the native NRAMP1-GFP under Mn excess, i.e. mainly TGN/EE (Figure S5, compare with Figure S3). This indicates that mimicking constitutive phosphorylation accelerates NRAMP1 endocytosis without altering its route within the endocytic pathway. These results strongly support the view that phosphorylation of one or several of the serines at positions 20, 22 and 24 is a prerequisite for NRAMP1 removal from the PM in response to Mn exposure.

Endocytosis of NRAMP1 regulates Mn uptake

We next investigated whether interfering with Mn mediated-endocytosis of NRAMP1 alters Mn homeostasis *in planta*. To that aim, the tolerance to Mn of the transgenic lines expressing GFP fusions with either NRAMP1 or the $S_{20,\ 22,\ 24}$A and $S_{20,\ 22,\ 24}$D isoforms was tested in Mn-replete hydroponic cultures. We reasoned that stabilization of NRAMP1 at the PM by the phosphodead mutations should result in Mn toxicity symptoms, whereas the phosphomimetic mutations should not. When Mn was present in the medium, young leaves of NRAMP1 $S_{20,\ 22,\ 24}$A-GFP expressing plants were crumpled and developed whitish veins (Figure 4k, l), phenotypic features that were not present in Mn-free medium (Figure 4e, f). This phenotype was not observed in the $S_{20,\ 22,\ 24}$D plants, nor in any other genotype of the experiment (Figure 4g-j). A similar phenotype with crumpled leaves and white veins was observed for $S_{20,\ 22,\ 24}$A plants in soil (Figure S6a) and is reminiscent of Mn toxicity symptoms (Li *et al.*, 2019). Furthermore, plant growth in agar plates in the presence of a high amount of Mn (750µM) was dramatically impaired by the $S_{20,\ 22,\ 24}$A, - but not the $S_{20,\ 22,\ 24}$D-, mutation (Figure S6b). Together these data suggest that stabilizing NRAMP1

at the plasma membrane results in decreased tolerance of the plant to Mn excess. We therefore concluded that NRAMP1 cycling represents an efficient means for the plant to ensure appropriate Mn uptake and prevent Mn toxicity.

Serine 20 controls NRAMP1 internalization

To identify among the three serines at positions 20, 22 and 24 which one(s) is(are) responsible for triggering NRAMP1 endocytosis, the three residues have been mutated individually. Transgenic plants expressing a GFP fusion with either one of the NRAMP1 mutant isoforms $S_{20}A$, $S_{20}D$, $S_{22}A$, $S_{22}D$, $S_{24}A$ and $S_{24}D$ were obtained and grown in Mn-deficient conditions prior to being exposed to 2mM Mn for 1h to induce internalization of the protein. Confocal microscopy observation revealed that $S_{20}A$ mutation, but not $S_{22}A$ nor $S_{24}A$, resulted in stabilization of NRAMP1 to the PM (Figure 5a-h), mimicking exactly the behavior of the $S_{20,\ 22,\ 24}A$ variant (Figure 3). Consistently, the phosphomimetic mutation $S_{20}D$ exacerbated the amount of internalized NRAMP1-GFP protein regardless of Mn supply (Figure 5i-j), as observed for the $S_{20,\ 22,\ 24}D$ variant. $S_{22}D$ and $S_{24}D$ mutations did not impact the cellular distribution of NRAMP1 (Figure S7). Therefore, there seems to be no cooperativity between Ser20, Ser22 and Ser24 to target NRAMP1 for endocytosis. On the contrary, phosphorylation of Ser20 alone appears to be necessary and sufficient for triggering the removal of NRAMP1 from the PM.

Discussion

With this study we aimed to better understand how plants maintain Mn homeostasis by controlling Mn entry within root cells through the high affinity Mn transporter NRAMP1. We demonstrated that proper regulation of Mn uptake by NRAMP1 is essential for plant health and that it primarily relies on the control of its trafficking between PM and endosomes. We further characterized the molecular mechanisms of this dynamics by showing that Mn-induced endocytosis of NRAMP1 is a clathrin-mediated process triggered by phosphorylation of the transporter.

We described in previous reports that *NRAMP1* transcription is poorly responsive to variation in Mn availability (Cailliatte *et al.*, 2010; Castaings *et al.*, 2016), which prompted us to investigate whether NRAMP1 could be regulated post-transcriptionally. Indeed, we show here that fine-tuning of Mn uptake mostly involves post-translational reallocation of the existing NRAMP1 protein pool exposed at the cell surface to different intracellular sites. Under Mn deficiency,

NRAMP1 is almost exclusively targeted to the PM where it performs Mn uptake, whereas under Mn excess it is rapidly internalized, thus preventing excessive entry of Mn and cytotoxicity (Figure 1). Substrate-induced internalization has been shown to regulate plant transporters such as the rice Mn transporter OsNRAMP3 or the Arabidopsis Fe and B transporters IRT1 and BOR1, respectively, all of which are then being targeted to the vacuole for degradation (Dubeaux *et al.*, 2018; Takano *et al.*, 2010; Yamaji *et al.*, 2013). NRAMP1 is thought to be turned-over by degradation in the vacuole as suggested by the accumulation of NRAMP1-GFP proteins in that compartment upon concanamycin A treatment (Agorio *et al.*, 2017). However, whether Mn does promote this degradation is still unknown. Indeed, we unexpectedly found no decrease in NRAMP1 steady state level upon a prolonged Mn exposure (Figure S1). This suggests that NRAMP1-GFP stability is high and that Mn triggers NRAMP1 internalization but does not impact the sorting of NRAMP1-containing endosomes to the vacuole. Once internalized, NRAMP1 appears to remain in endosomal membranes, ready to be sorted back to the PM in response to Mn shortage. Thus, in these conditions, cycling of NRAMP1 polypeptides takes a short route, likely allowing a quick adaptation of Mn uptake to versatile Mn needs. This dynamic cycling of NRAMP1 between PM and endosomal compartments is what allows the plant permissiveness to relatively high Mn concentrations. This is evidenced by the observation that plant tolerance to Mn dramatically decreases when NRAMP1 is stabilized at the PM by the SA phosphodead mutations. It unequivocally demonstrates that regulating NRAMP1 membrane trafficking in response to Mn availability is of utmost importance to allow adaptation to fluctuating Mn availability in soils.

We further show here that Mn-induced internalization of NRAMP1 involves the major clathrin-dependent endocytic pathway since impairing CME stabilizes NRAMP1 at the PM regardless of the Mn regime. The Auxilin-Like 2 overexpressing line that we used to inhibit CME, which produces a larger amount of clathrin uncoating factor, appears to be specific for the PM pool of clathrin and does not impact clathrin coating of endosomal compartments (Adamowski *et al.*, 2018). Therefore, the finding that NRAMP1 internalization is inhibited in this line enabled to establish the involvement of the clathrin pathway in the early step of NRAMP1 trafficking from the PM to early endosomes.

Our results demonstrate that phosphorylation is a prerequisite for Mn-induced CME of NRAMP1. Indeed, preventing phosphorylation of three serine residues in the N-terminal cytosol-exposed tail of the transporter stabilizes the protein at the PM and abolishes its endocytosis in response to Mn.

This is further confirmed by a phosphomimetic NRAMP1 variant, which shows the opposite behavior, i.e. entirely addressed in endosomes and almost undetectable at the PM regardless of the Mn regime. A possible explanation could be that the SD mutations impair PM targeting of NRAMP1. The fact that the phosphomimetic variant rescues tolerance of the *nramp1* mutant to Mn deficiency however suggests that it is correctly addressed to the PM but that its cycling between PM and endosomes is accelerated. Moreover, among the trio of serines 20, 22 and 24, we were able by mutating them individually to pinpoint a unique serine residue at position 20 which must be phosphorylated in order for Mn-induced NRAMP1endocytosis to occur. Phosphorylation is well-known for playing important roles in protein trafficking. Yet, to our knowledge, it has not been reported to directly promote CME of plant PM transporters. Instead, internalization of the transporter requires either ubiquitination alone or the combination of phosphorylation and ubiquitination. For instance, in response to an excess of its metal substrates, the IRT1 transporter is phosphorylated by the CIPK23 kinase, which promotes its polyubiquitination in endosomes and subsequent sorting to the vacuole for degradation (Dubeaux *et al.*, 2018). Although the amount of IRT1 polypeptides present at the PM increases in a *cipk23* mutant, there is no compelling evidence that phosphorylation triggers endocytosis. Rather, the lack of vacuolar sorting of IRT1 in *cipk23* may result in enlarging the pool of IRT1-containing endosomes, which would then recycle IRT1 back to the PM. A recent study suggests that phosphorylation of IRT1 likely dissociates IRT1 from its PM-located complex with the ferric reductase FRO2 and the H^+-ATPase AHA2 prior to its monoubiquitination and internalization (Martin Barranco, 2020). The scenario seems different for NRAMP1 where phosphorylation affects the very early step of endocytosis from the PM since 1) this route is interrupted in the PM endocytosis impaired-auxilin overexpressor, 2) NRAMP1 phosphodead mutant was unable to move out of the PM and displayed high sensitivity to Mn, 3) phosphomimetic mutants are constitutively endocytosed from the PM. Whether phosphorylation of NRAMP1 helps recruiting a specific ubiquitin ligase for further sorting will be important to investigate.

Given that phosphorylation of NRAMP1 triggers endocytosis and that endocytosis occurs specifically in response to Mn exposure, the question arises whether NRAMP1 phosphorylation is stress-induced. In the case of Smf1p, the yeast homolog of NRAMP1, endocytosis occurs in response to cadmium and requires a step of phosphorylation, like NRAMP1 (Nikko et al., 2008). Nevertheless, phosphorylation of Smf1p is not the trigger for its Cd-induced endocytosis since a

phosphomimetic mutation is still subject to control by cadmium. Therefore, Smf1p phosphorylation likely helps recruiting the ubiquitin machinery that promotes its removal from the PM (Nikko *et al.*, 2008). Unlike Smf1p, Mn-responsive endocytosis of NRAMP1 is disrupted in the SD mutation and the protein is constitutively endocytosed. This indicates that phosphorylation is the trigger of its endocytosis and strongly suggests that it is induced by Mn.

Active cycling of root transporters between PM and endomembrane compartments appears to control their activity of transport by maintaining a polar distribution of the proteins at the cell surface, i.e. importers facing the soil and exporters facing the stele (Barberon *et al.*, 2014; Takano *et al.*, 2010; Ma and Yamaji , 2008;; Yamaji *et al.*, 2013; Wang *et al.*, 2017). NRAMP1 does not show a polar localization when expressed under the CaMV *35S* constitutive promoter. Instead it is evenly distributed at the PM of all root cells. The strong and ubiquitous expression driven by the 35S promoter may mask or bypass polar targeting of a PM protein. Polarity of transporters is thought to be an efficient way to drive nutrients uptake across the root cell layers from the soil to the vascular tissues. In the case of Mn it has been shown in rice that Mn translocation to the stele depends on two transporters oppositely distributed at the surface of endodermal cells, namely OsNRAMP5 promoting Mn uptake on the distal side and the efflux transporter OsMTP9 secreting Mn at the proximal side towards the vasculature (Ueno *et al.*, 2015). Given that NRAMP1 is expressed in all cell layers especially in endodermis (Cailliatte *et al.*, 2010), it is tempting to speculate that NRAMP1 and its yet unknown efflux transporter counterpart may also display such a polarity. An argument in favor comes from a study of the impact of nutrient availability on the extent of suberization of the endodermis (Barberon *et al.*, 2016). Interestingly, in the *nramp1* mutant, suberization becomes patchy, likely to allow entry of Mn ions in the stele in the absence of NRAMP1. This supports an important role of NRAMP1 in Mn uptake by root endodermal cells and raises the possibility that it is outwardly distributed in the PM to allow radial transport towards the vascular tissue of the root. In summary our findings show that Mn entry into the root is tightly controlled through the Mn-regulated, dynamic removal of the NRAMP1 transporter from the PM. We show here that the trigger for NRAMP1 endocytosis is a phosphorylation event. The finding that impairing such phosphorylation dramatically reduces the plant tolerance to Mn excess stresses the importance of regulating Mn uptake in the face of fluctuating availability of this nutrient in soils and undermines the dogma in which Mn is only marginally toxic to plants, hence requiring little control of its uptake.

Experimental procedures

Plant material. The *A. thaliana* mutant *nramp1-1* (SALK_053236) and the transgenic line *nramp1-1 NRAMP1-GFP #8* (*NRAMP1-GFP* in the text) expressing NRAMP1-GFP protein under the control of the constitutive 35S promoter in the *nramp1-1* background were described in (Cailliatte et al., 2010). The previously published transgenic line *XVE»AUXILIN-LIKE2* (Adamowski et al., 2018), expressing the *AUXILIN-LIKE2* gene under the control of an estradiol inducible promoter, was crossed with the *nramp1-1 NRAMP1-GFP* line. *nramp1-1 NRAMP1-GFP AUXILIN-LIKE2* homozygote plants were selected by PCR.

Cloning of NRAMP1-GFP serine variants and expression in transgenic plants. NRAMP1 coding sequences without stop codons and harboring mutations in the serines 20, 22 and 24 to alanines ($S_{20, 22, 24}A$) or to aspartic acids ($S_{20, 22, 24}D$) were obtained by PCR-based site-directed mutagenesis using the following primer sets 5'-ATGGCGGCTACAGGATCTG-3'/5'-AgccTTCgccAATgcgCCACTC-3' and 5'-GAGTGGcgcATTggcGAAggcT-3' /5'-TCAGTCAACATCGGAGGTA-3' for $S_{20, 22, 24}A$ and 5'-ATGGCGGCTACAGGATCTG-3'/5'-AgacTTCgacAATgatCCACTC-3' and 5'-GAGTGGatcATTgtcGAAgtcT-3/'5'-TCAGTCAACATCGGAGGTA-3' for $S_{20, 22, 24}D$ (lower case letters indicate mutation sites). PCR fragments were then cloned using the Gateway® technology (Invitrogen™, Thermo Fisher Scientific) in the entry vector pDONR207 by BP reactions and subcloned by LR reactions in the destination vector pGWB5 allowing constitutive expression of NRAMP1-GFP variants in plants. The two constructs (pGWB5 NRAMP1 S $S_{20, 22, 24}A$ and pGWB5 NRAMP1 S $S_{20, 22, 24}D$) were introduced in *Agrobacterium tumefaciens* strain GV3101 and transformed in *nramp1-1* mutant plants by floral dip (Clough and Bent, 1998). Homozygote plants were selected based on their resistance to hygromycine.

Growth conditions. For imaging experiments, plants were grown for one week under long days (21.5 °C, 16 h light/8 h dark) either on ½ MS, 1% sucrose agar plates with limited Mn (≈ 0,2 µM Mn traces brought by the agar, +/-Mn) or standard Mn (20 µM $MnSO_4$, +Mn) or in ½ MS, 1% sucrose liquid medium with no added Mn (0 Mn) or standard Mn (20 µM $MnSO_4$, +Mn). For phenotyping experiments, plants were grown for three weeks hydroponically under short days (8 h

light/ 16 h dark, 21 °C) in a previously described nutrient solution (Castaings *et al*., 2016) without added Mn (-Mn) or 20 µM $MnSO_4$ (+Mn).

Mn excess treatment, estradiol transgene induction and FMF-64 staining. For Mn excess treatment, 7 days-old Mn- starved or Mn-deficient seedlings were incubated 1 h in liquid ½ MS medium containing 2 mM $MnSO_4^-$, 1% sucrose and 100 µM cycloheximide (CHX, Sigma Aldrich) and mounted in the same medium on microscopy slides before imaging.

For *AUXILIN-LIKE2* transgene induction, 6 days-old seedlings grown on Mn-depleted ½ MS vertical agar plates were transferred on the same plates supplemented with 3 mg. l^{-1} estradiol for 20 h. Seedlings were stained 5 min with 10 µM FM4-64 before imaging.

Confocal imaging and fluorescence quantification. Epidermal, cortical and endodermal root cells from the division and elongation zone were imaged on an inverted Leica SP8 confocal microscope with a 40 × /1.1 water objective and with the following excitation and detection wavelengths, respectively: 488 nm and 500–540 nm for GFP and 561 nm and 580-630 nm for FM4-64. Dual-color images of GFP and FM4-64 were acquired with the best lateral and axial resolution (pixel size, 70 nm) by sequential line mode allowing the separation of channels by both excitation and emission. NRAMP1-GFP PM signal intensities were quantified by measuring the mean grey values of segmented lines (1-pixel wide) drawn along multiple PMs in individual microscopic pictures using ImageJ.

Data availability statement

All relevant data can be found within the manuscript and its supporting materials

Acknowledgements

We thank Jiri Friml and Alexandre Martinière for providing us with the *XVE»AUXILIN-LIKE2* and *PIN2::PIN2-GFP* expressing line, respectively. Work was funded by the Agence Nationale pour la Recherche through the French-Taiwanese bilateral ANR grant MANOMICS (ANR-2011-ISV6-001-01) and the ANR grant DEFIMAN (ANR-19-CE20-0009), by the Centre National de la Recherche Scientifique and by the Institut National de la Recherche Agronomique. We acknowledge the imaging facility MRI, member of the national infrastructure France-BioImaging infrastructure supported by the French National Research Agency (ANR-10-INBS-04,

«Investments for the future"). C.C. and C.A. were supported by the Centre National de la Recherche Scientifique. L.C., T.K. and D.C. were supported by the University of Montpellier (France).

Author contributions

L.C., C.A., T.K. and D.C conducted the experiments. L.C. analyzed the data. L.C. and C.C. designed and supervised the study, and wrote the manuscript.

Conflict of interest

The authors declare no conflict of interest.

Supporting legends

Supporting Figure 1. Mn does not affect NRAMP1 protein abundance.
Immunoblot analysis of NRAMP1-GFP protein accumulation in NRAMP1-GFP transgenic plants grown for 7 days in Mn-free liquid medium and treated with 2 mM Mn (++Mn) or 0 mM Mn (-Mn) for 0, 3 h, 6 h and 24 h in the presence of 100µM cycloheximide. NRAMP1-GFP protein was revealed with anti-GFP antibodies. The membrane was stripped and blotted again with anti-Actin antibodies.

Supporting Figure 2. Mn excess specifically triggers NRAMP1 endocytosis.
Confocal imaging of roots of transgenic lines expressing NRAMP1-GFP fusion (top lane) or PIN2-GFP fusion (bottom lane). Plants were grown for 7 days in Mn-free liquid medium (-Mn) and resupplied with 2 mM Mn for 1h (++Mn) in the presence of 100µM cycloheximide. Scale bars = 20 µm.

Supporting Figure 3. NRAMP1-GFP is sorted to endosomal compartments under Mn excess.
Confocal microscopy observations of root cells from 7 day-old plants grown on Mn-limited medium (0.2 µM, +/-Mn) and exposed 1h to 2mM Mn and 100µM CHX (++Mn).
(a) Plants co-expressing NRAMP1-GFP and the TGN/EE marker mCherry-VTI12**.**
(b) Plants co-expressing NRAMP1-GFP and the TGN/EE and MVB/LE marker mCherry-ARA7. Pearson's (r_p) correlation coefficients are shown. Scale bars = 10 µm.

Supporting Figure 4. Mapping of NRAMP1 phosphorylated sites.

(a) NRAMP1 amino acid sequence with putative transmembrane domains highlighted in grey, predicted phosphorylated residues in green and experimentally-found phosphorylated residues in red as shown in the PhosPhAt database (http://phosphat.uni-hohenheim.de).

(b) NRAMP1 protein topology with transmembrane domains highlighted in grey, predicted phosphorylated residues marked with green asterisks and experimentally found phosphorylated residues with red asterisks.

Supporting Figure 5. NRAMP1 $S_{20, 22, 24}$D-GFP is constitutively internalized.

Confocal microscopy observations of root cells from 7 days-old plants grown on Mn-limited medium (0.2 µM, +/-Mn) and exposed 1h to 2mM Mn and 100µM CHX (++Mn).

(a) Plants co-expressing NRAMP1 $S_{20, 22, 24}$D-GFP and the TGN/EE marker mCherry-VTI12**. (b)** Plants co-expressing NRAMP1 $S_{20, 22, 24}$D-GFP and the TGN/EE and MVB/LE marker mCherry-ARA7. Pearson's (r_p) correlation coefficients are shown. Scale bars = 10 µm.

Supporting Figure 6. NRAMP1 $S_{20, 22, 24}$A-GFP expression results in hypersensitivity to Mn.

Complementation test of the *nramp1-1* plants by the NRAMP1-GFP, NRAMP1 $S_{20, 22, 24}$D-GFP or NRAMP1 $S_{20, 22, 24}$A-GFP constructs. Plants were grown on soil for 3 weeks **(a)** or *in vitro* on agar plates for 10 days without added Mn (-Mn), standard 20µM Mn (+Mn) or an excess of 750µM Mn (++Mn) **(b)**.

Supporting Figure 7. Phosphorylation of serine 20 triggers NRAMP1 endocytosis.

Confocal imaging of roots of transgenic lines expressing a GFP fusion with either NRAMP1 **(a, b)**, NRAMP1 S_{20}D **(c, d)**, NRAMP1 S_{22}D **(e, f)** or NRAMP1 S_{24}D **(g, h)** isoforms. Plants were grown for 7 days in Mn-limited medium (0.2 µM, +/-Mn) and either resupplied **(b, d, f, h)** or not **(a, c, e, g)** with an excess (2 mM) of Mn for 1h (++Mn). Scale bars = 10 µm.

References

Adamowski, M., Narasimhan, M., Kania, U., Glanc, M., De Jaeger, G. and Friml, J. (2018) A Functional Study of AUXILIN-LIKE1 and 2, Two Putative Clathrin Uncoating Factors in Arabidopsis. *Plant Cell,* **30**, 700-716.

Agorio, A., Giraudat, J., Bianchi, M.W., Marion, J., Espagne, C., Castaings, L., Lelievre, F., Curie, C., Thomine, S. and Merlot, S. (2017) Phosphatidylinositol 3-phosphate-binding protein

AtPH1 controls the localization of the metal transporter NRAMP1 in Arabidopsis. *Proc. Natl Acad. Sci. USA*, **114**, E3354-E3363.

Barberon, M., Zelazny, E., Robert, S., Conéjéro, G., Curie, C., Friml, J., Vert, G. (2011) Monoubiquitin-dependent endocytosis of the iron-regulated transporter 1 (IRT1) transporter controls iron uptake in plants. *Proc. Natl Acad. Sci. USA*, **108**, E450-458.

Barberon, M., Dubeaux, G., Kolb, C., Isono, E., Zelazny, E. and Vert, G. (2014) Polarization of IRON-REGULATED TRANSPORTER 1 (IRT1) to the plant-soil interface plays crucial role in metal homeostasis. *Proc. Natl Acad. Sci. USA*, **111**, 8293-8298.

Barberon, M., Vermeer, J.E., De Bellis, D., Wang, P., Naseer, S., Andersen, T.G., Humbel, B.M., Nawrath, C., Takano, J., Salt, D.E. and Geldner, N. (2016) Adaptation of root function by nutrient-induced plasticity of endodermal differentiation. *Cell*, **164**, 447-459.

Cailliatte, R., Schikora, A., Briat, J.F., Mari, S. and Curie, C. (2010) High-affinity manganese uptake by the metal transporter NRAMP1 is essential for Arabidopsis growth in low manganese conditions. *Plant Cell*, **22**, 904-917.

Castaings, L., Caquot, A., Loubet, S. and Curie, C. (2016) The high-affinity metal Transporters NRAMP1 and IRT1 Team up to Take up Iron under Sufficient Metal Provision. *Sci. Rep.*, **6**, 37222.

Clough, S.J. and Bent, A.F. (1998) Floral dip: a simplified method for Agrobacterium-mediated transformation of Arabidopsis thaliana. *Plant J.*, **16**, 735-743.

de Varennes, A., Carneiro, J.P. and Goss, M.J. (20001) Characterization of manganese toxicity in two species of annual medics. *J. Plant Nutr.*, **24**, 1947-1955.

Dubeaux, G., Neveu, J., Zelazny, E. and Vert, G. (2018) Metal Sensing by the IRT1 Transporter-Receptor Orchestrates Its Own Degradation and Plant Metal Nutrition. *Mol. Cell*, **69**, 953-964 e955.

Eguez, L., Chung, Y.S., Kuchibhatla, A., Paidhungat, M. and Garrett, S. (2004) Yeast Mn^{2+} transporter, Smf1p, is regulated by ubiquitin-dependent vacuolar protein sorting. *Genetics*, **167**, 107-117.

Eide, D., Broderius, M., Fett, J. and Guerinot, M.L. (1996) A novel iron-regulated metal transporter from plants identified by functional expression in yeast. *Proc. Natl Acad. Sci. USA*, **93**, 5624-5628.

Foot, N.J., Dalton, H.E., Shearwin-Whyatt, L.M., Dorstyn, L., Tan, S.S., Yang, B., Kumar, S. (2008) Regulation of the divalent metal ion transporter DMT1 and iron homeostasis by a ubiquitin-dependent mechanism involving Ndfips and WWP2. *Blood,* **15**, 4268-4275.

Geldner, N., Denervaud-Tendon, V., Hyman, D.L., Mayer, U., Stierhof, Y.D. and Chory, J. (2009) Rapid, combinatorial analysis of membrane compartments in intact plants with a multicolor marker set. *Plant J.*, **59**, 169-178.

Geszvain, K., Butterfield, C., Davis, R.E., Madison, A.S., Lee, S.W., Parker, D.L., Soldatova, A., Spiro, T.G., Luther, G.W. and Tebo, B.M. (2012) The molecular biogeochemistry of manganese(II) oxidation. *Biochem. Soc. Trans.*, **40**, 1244-1248.

Horst, W. (1988) The physiology of manganese toxicity. *Manganese in soils and plants (R.D. Graham, R.J. Hannam and N.C. Uren, eds.) Kluwer Academic Publishers, Dordrecht* 175-188.

Ishimaru, Y., Suzuki, M., Tsukamoto, T., Suzuki, K., Nakazono, M., Kobayashi, T., Wada, Y., Watanabe, S., Matsuhashi, S., Takahashi, M., Nakanishi, H., Mori, S. and Nishizawa, N.K. (2006) Rice plants take up iron as an Fe3+-phytosiderophore and as Fe2+. *Plant J.*, **45**, 335-346.

Ishimaru, Y., Takahashi, R., Bashir, K., Shimo, H., Senoura, T., Sugimoto, K., Ono, K., Yano, M., Ishikawa, S., Arao, T., Nakanishi, H. and Nishizawa, N.K. (2012) Characterizing the role of rice NRAMP5 in Manganese, Iron and Cadmium Transport. *Sci. Rep.*, **2**, 286.

Ito, E., Uemura, T., Ueda, T. and Nakano, A. (2016) Distribution of RAB5-positive multivesicular endosomes and the trans-Golgi network in root meristematic cells of Arabidopsis thaliana. *Plant Biotechnol (Tokyo)*, **33**, 281-286.

Kasai, K., Takano, J., Miwa, K., Toyoda, A., Fujiwara, T. (2011) High boron-induced ubiquitination regulates vacuolar sorting of the BOR1 borate transporter in *Arabidopsis thaliana*. *J. Biol. Chem.,* **286,** 6175-3183.

Li, J., Jia, Y., Dong, R., Huang, R., Liu, P., Li, X., Wang, Z., Liu, G. and Chen, Z. (2019) Advances in the Mechanisms of Plant Tolerance to Manganese Toxicity. *Int. J. Mol. Sci.*, **20**.

Lieser, S.A., Davis, T.C., Helmann, J.D. and Cohen, S.M. (2003) DNA-binding and oligomerization studies of the manganese(II) metalloregulatory protein MntR from Bacillus subtilis. *Biochemistry*, **42**, 12634-12642.

Lin, W.Y., Huang, T.K., Chiou, T.J. (2013) Nitrogen limitation adaptation, a target of microRNA827, mediates degradation of plasma membrane-localized phosphate transporters to maintain phosphate homeostasis in Arabidopsis. *Plant Cell*, **10**, 4061-4074.

Liu, X.F. and Culotta, V.C. (1999) Post-translation control of Nramp metal transport in yeast. Role of metal ions and the BSD2 gene. *J. Bio. Chem.*, **274**, 4863-4868.

Long, L., Persson, D.P., Duan, F., Jorgensen, K., Yuan, L., Schjoerring, J.K. and Pedas, P.R. (2018) The iron-regulated transporter 1 plays an essential role in uptake, translocation and grain-loading of manganese, but not iron, in barley. *New Phytol.*, **217**, 1640-1653.

Ma, J.F. and Yamaji, N. (2008) Functions and transport of silicon in plants. *Cell. Mol. Life Sci.*, **65**, 3049-3057.

Marschner, P. (2012) Function of nutrients: micronutrients. *Mineral Nutrition of Higher Plants, 3rd ed., Academic Press: Boston, MA, USA*, **Chapter 7**, 191-248.

Martin-Barranco, A., Spielmann, J., Dubeaux, G., Vert, G., Zelazny, E. (2020) Dynamic Control of the High-Affinity Iron Uptake Complex in Root Epidermal Cells. *Plant Physiol.*, **3**, 1236-1250.

Nikko, E., Sullivan, J.A. and Pelham, H.R. (2008) Arrestin-like proteins mediate ubiquitination and endocytosis of the yeast metal transporter Smf1. *EMBO Rep*, **9**, 1216-1221.

Papp-Wallace, K.M. and Maguire, M.E. (2006) Manganese transport and the role of manganese in virulence. *Annu. Rev. Microbiol.*, **60**, 187-209.

Pedas, P., Hebbern, C.A., Schjoerring, J.K., Holm, P.E. and Husted, S. (2005) Differential capacity for high-affinity manganese uptake contributes to differences between barley genotypes in tolerance to low manganese availability. *Plant Physiol.*, **139**, 1411-1420.

Sasaki, A., Yamaji, N., Yokosho, K. and Ma, J.F. (2012) Nramp5 is a major transporter responsible for manganese and cadmium uptake in rice. *Plant Cell*, **24**, 2155-2167.

Schmidt, S.B., Jensen, P.E. and Husted, S. (2016) Manganese Deficiency in Plants: The Impact on Photosystem II. *Trends Plant Sci.*, **21**, 622-632.

Shin, L.J., Lo, J.C., Chen, G.H., Callis, J., Fu, H., Yeh, K.C. (2013) IRT1 degradation factor1, a ring E3 ubiquitin ligase, regulates the degradation of iron-regulated transporter1 in Arabidopsis. *Plant Cell*, **8**, 3039-3051.

Sparrow, L.A. and Uren, N.C. (2014) Manganese oxidation and reduction in soils: effects of temperature, water potential, pH and their interactions. *Soil Research*, **52**, 483-494.

Stimpson, H.E., Lewis, M.J. and Pelham, H.R. (2006) Transferrin receptor-like proteins control the degradation of a yeast metal transporter. *EMBO J.*, **25**, 662-672.

Takano, J., Tanaka, M., Toyoda, A., Miwa, K., Kasai, K., Fuji, K., Onouchi, H., Naito, S. and Fujiwara, T. (2010) Polar localization and degradation of Arabidopsis boron transporters through distinct trafficking pathways. *Proc. Natl Acad. Sci. USA*, **107**, 5220-5225.

Ueno, D., Sasaki, A., Yamaji, N., Miyaji, T., Fujii, Y., Takemoto, Y., Moriyama, S., Che, J., Moriyama, Y., Iwasaki, K. and Ma, J.F. (2015) A polarly localized transporter for efficient manganese uptake in rice. *Nat. Plants*, **1**, 15170.

Vert, G., Grotz, N., Dedaldechamp, F., Gaymard, F., Guerinot, M.L., Briat, J.F. and Curie, C. (2002) IRT1, an Arabidopsis Transporter Essential for Iron Uptake from the Soil and for Plant Growth. *Plant Cell*, **14**, 1223-1233.

Wang, S., Yoshinari, A., Shimada, T., Hara-Nishimura, I., Mitani-Ueno, N., Feng Ma, J., Naito, S., Takano, J. (2017) Polar Localization of the NIP5;1 Boric Acid Channel Is Maintained by Endocytosis and Facilitates Boron Transport in Arabidopsis Roots.*Plant Cell*, **4**, 824-842.

Wu, D., Yamaji, N., Yamane, M., Kashino-Fujii, M., Sato, K. and Feng Ma, J. (2016) The HvNramp5 Transporter Mediates Uptake of Cadmium and Manganese, But Not Iron. *Plant Physiol.*, **172**, 1899-1910.

Yamaji, N., Sasaki, A., Xia, J.X., Yokosho, K. and Ma, J.F. (2013) A node-based switch for preferential distribution of manganese in rice. *Nat. Commun.*, **4**, 2442.

Yanatori, I. and Kishi, F. (2019) DMT1 and iron transport. *Free Radic. Biol. Med.*, **133**, 55-63.

Figure legends

Figure 1. Manganese controls membrane localization of NRAMP1.

Confocal microscopy observations of root cells from NRAMP1-GFP transgenic plants grown 7 days in liquid medium **(a, d)** with 20 µM Mn (+ Mn) or **(b, e)** without Mn (0 Mn). **(c, f)** Plants grown without Mn were then exposed 1h to 2mM Mn prior to the observation (++ Mn). **(g)** Box plot representation of plasma membrane signals intensity from root cells of plant grown with 20 µM Mn (+ Mn, n= 88) or without Mn (0 Mn, n=83). Asterisks indicate significantly different data (T-test, p value <0,0001). Scale bars = 20 µm.

Figure 2. NRAMP1 is regulated by clathrin-mediated endocytosis.

The NRAMP1-GFP line was crossed with an oestradiol inducible XVE>>AUXILIN-LIKE 2 overexpressor line. Confocal microscopy observation of roots of 7 day-old plants grown in solid

medium with no added Mn, induced (**d-f**) or not (**a-c**) with oestradiol for 20 hours in order to promote AUXILIN-LIKE 2 expression, then exposed to 2 mM Mn and 100 µM CHX for 1h, and finally stained with FM4-64 for 5 min. (**a**, **d**) NRAMP1-GFP. (**b**, **e**) FM4-64. (**c**, **f**) Merged NRAMP1-GFP and FM4-64 signals. Scale bars = 10 µm.

Figure 3. NRAMP1 phosphorylation controls its internalization.

Confocal imaging of roots of NRAMP1-GFP **(a-b)**, NRAMP1 $S_{20,22,24}$A-GFP **(c-d)** or NRAMP1 $S_{20,22,24}$D-GFP **(e-f)** lines. Plants were grown for 7 days in solid medium under limited Mn supply (0.2 µM, +/- Mn), then exposed **(b, d, f)** or not **(a, c, e)** to 2 mM Mn during 1 hour (++Mn). All plants were treated 1 hour with 100 µM CHX before observation. Scale bars = 10 µm.

Figure 4. NRAMP1 cycling protects the plant against Mn toxicity.

Phenotype of the indicated genotypes grown for 3 weeks in hydroponic culture in the presence of 20 µM Mn (+Mn) (**a-e**) or without Mn (-Mn) (**g-k**). (**f**, **l**) Closeup views of young leaves of the NRAMP1 $S_{20,22,24}$A line grown in hydroponics without Mn (**f**) or with 20 µM Mn (**l**). Scale bars = 1 cm (**a-e**, **g-k**) or 0.5 cm (**f**, **l**).

Figure 5. Phosphorylation of serine 20 is crucial for NRAMP1 endocytosis.

Confocal imaging of roots of transgenic lines expressing a GFP fusion with either NRAMP1 **(a, b)**, NRAMP1 S_{20}A **(c, d)**, NRAMP1 S_{22}A **(e, f)**, NRAMP1 S_{24}A **(g, h)** or NRAMP1 S_{20}D **(i, j)** isoforms. Plants were grown for 7 days in Mn-limited solid medium (0.2 µM, +/-Mn) and either resupplied **(b, d, f, h)** or not **(a, c, e, g)** with an excess (2 mM) of Mn for 1h (++Mn) in the presence of 100µM CHX. Scale bars =10µm.

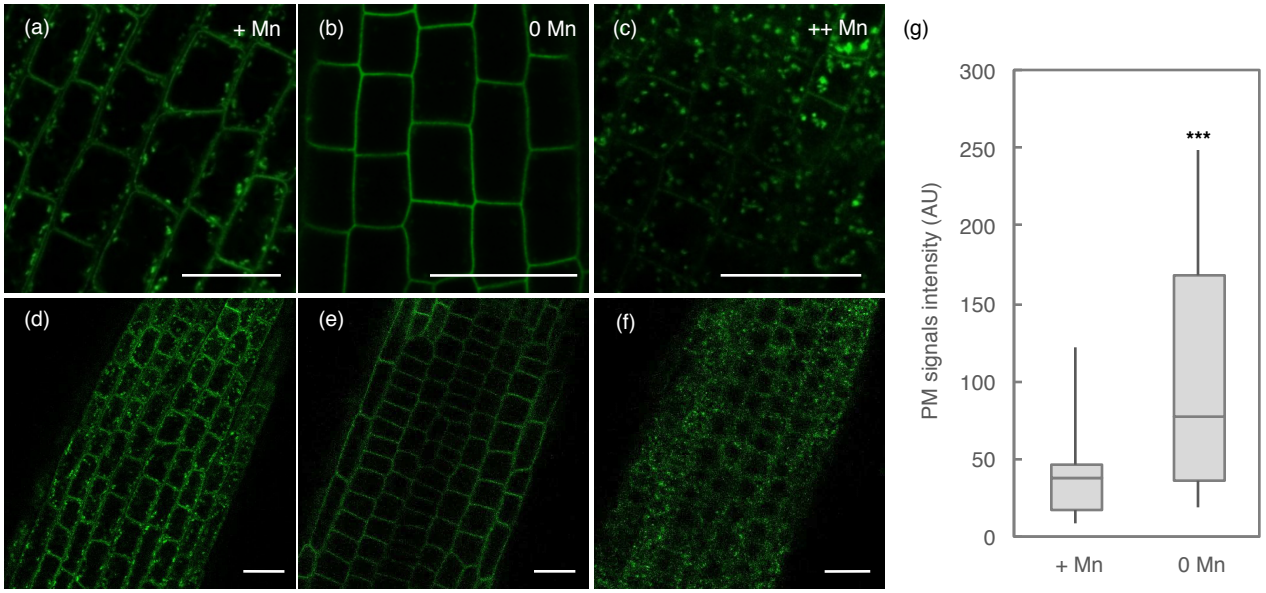
(a)
+ Mn
(b)
0 Mn
(c)
++ Mn
(d)
(e)
(f)
(g)
PM signals intensity (AU)
300
250
200
150
100
50
0
***
+ Mn
0 Mn

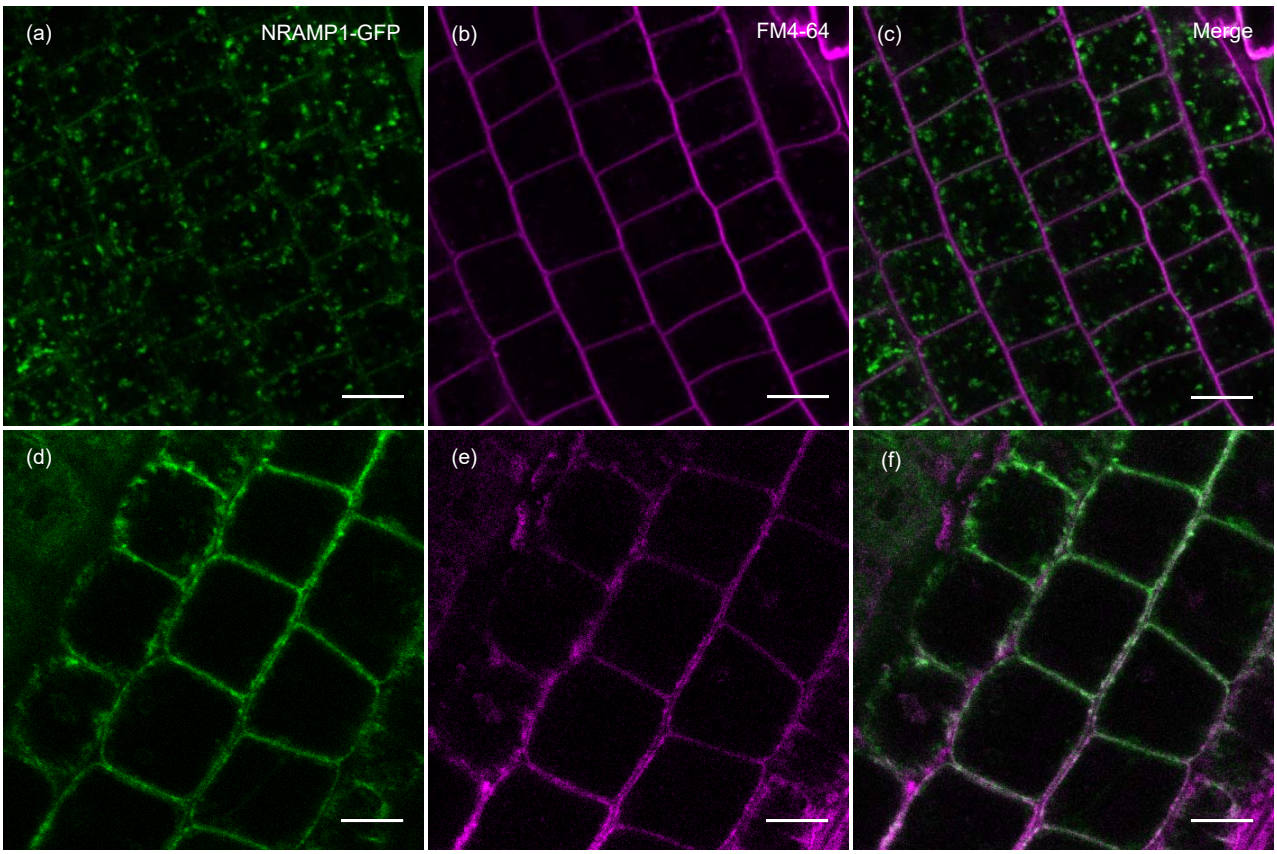
(a)
NRAMP1-GFP
(b)
FM4-64
(c)
Merge
(d)
(e)
(f)

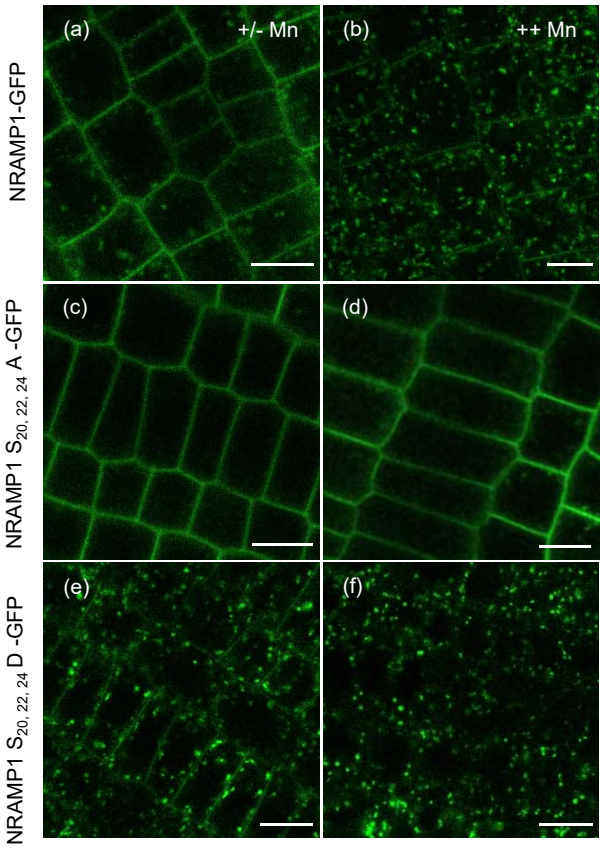
(a)
+/- Mn
(b)
++ Mn
NRAMP1-GFP
(c)
(d)
NRAMP1 S20, 22, 24 A -GFP
(e)
(f)
NRAMP1 S20, 22, 24 D -GFP

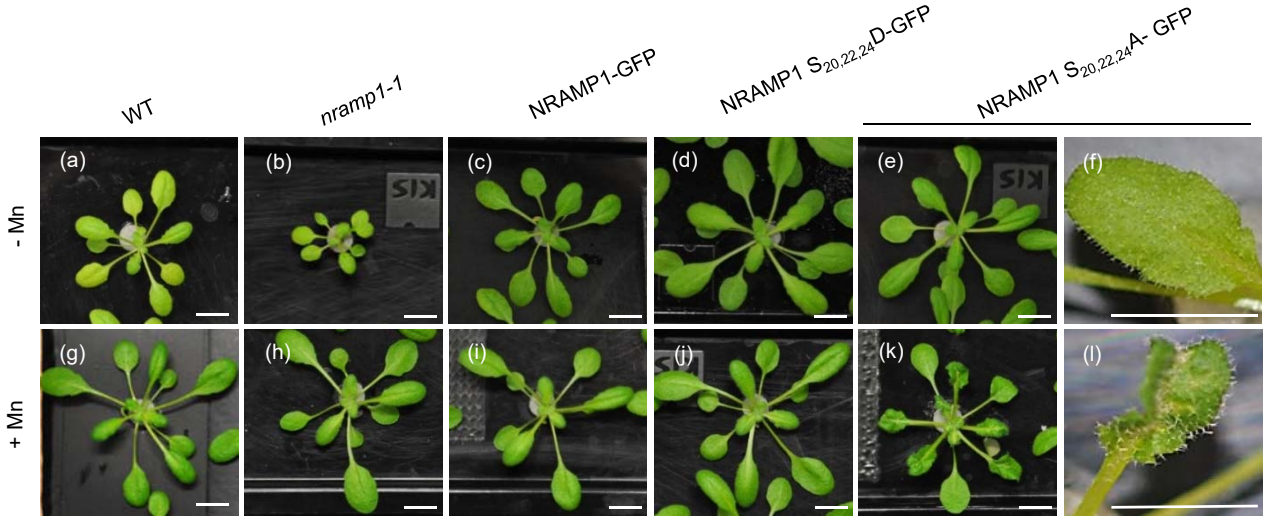
WT
nramp1-1
NRAMP1-GFP
NRAMP1 S20,22,24D-GFP
NRAMP1 S20,22,24A- GFP
- Mn
+ Mn
(a)
(b)
(c)
(d)
(e)
(f)
(g)
(h)
(i)
(j)
(k)
(l)

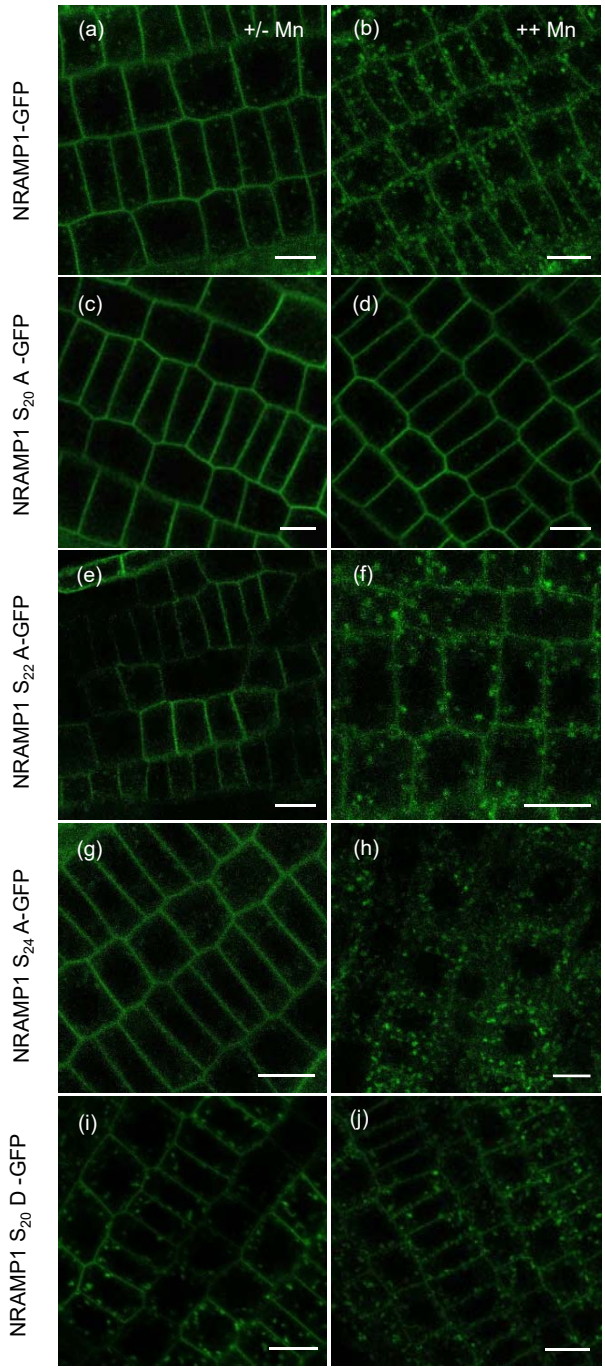
(a)
+/- Mn
(b)
++ Mn
NRAMP1-GFP
(c)
(d)
NRAMP1 S20 A -GFP
(e)
(f)
NRAMP1 S22 A-GFP
(g)
(h)
NRAMP1 S24 A-GFP
(i)
(j)
NRAMP1 S20 D -GFP